Chapter 8

REMOVAL OF CADMIUM USING NANO CRYSATLLINE IRON OXIDE/ HYDROXIDE

This chapter deals with the result of adsorption of cadmium on nano iron oxide/hydroxide. Effect of various parameters and their significance on removal (%) of cadmium is assessed. The isotherm and kinetic parameter determination by linear and nonlinear methods are assessed. Thermodynamic parameters were also determined for checking feasibility of adsorption.

8.1. Adsorption experiments

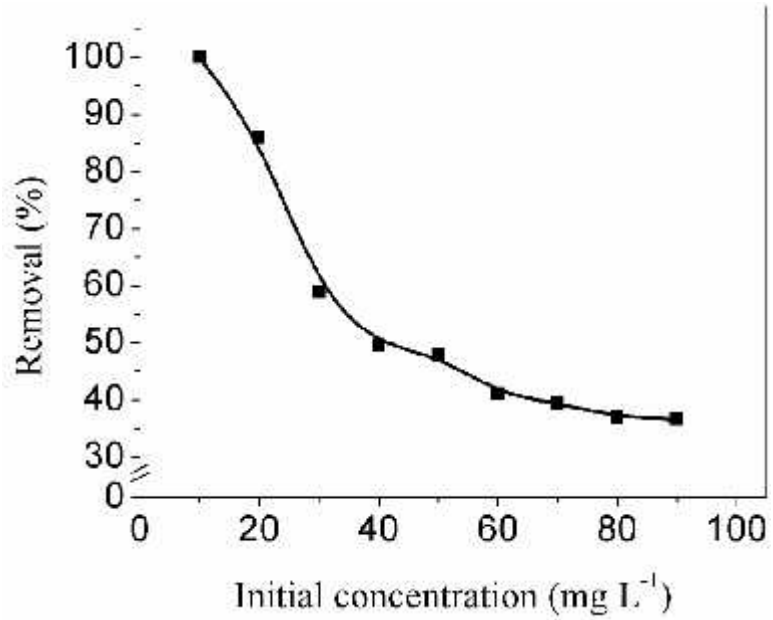

Figure 8.1 Effect of initial concentration on removal (%) of cadmium from aqueous solution on nano crystalline iron oxide/hydroxide (Initial pH= 6, adsorbent dose 2 g L^{-1}, Temperature 303 K)

Preliminary studies were conducted in the range of initial concentration 10 to 90 mg L^{-1} (Figure 8.1). The cadmium removal (%) decreased with increase of initial concentration and maximum removal was achieved at lowest initial concentration tested i.e.10 mg L^{-1}. In addition to this, cadmium removal (%) increased with increase of pH (Figure 8.2). At pH 2 there was no significant cadmium removal (%), hence the in RSM studies, pH 4 is taken as lower limit of pH. In study of effect of adsorbent dose, the cadmium removal (%) becomes stagnant after the adsorbent dose 5 g L^{-1}. Hence the adsorbent dose is taken as 4 g L^{-1}. In case of effect of contact time on cadmium removal (%); the cadmium

removal (%) becomes stagnant and equilibrium is reached in 20 min. Hence, all experiments were conducted for 20 min.

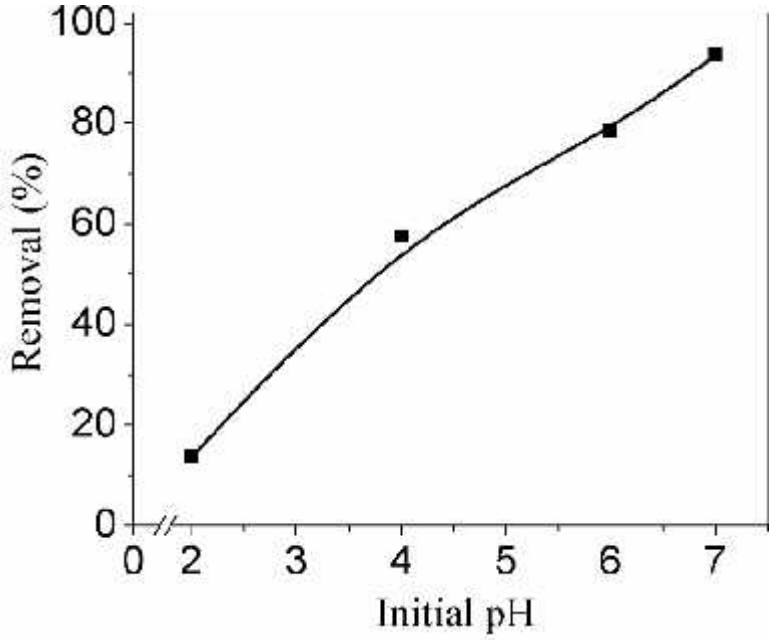

Figure 8.2 Effect of initial pH on removal (%) of cadmium from aqueous solution on nano crystalline iron oxide/hydroxide (Initial concentration= 20 mg L^{-1}, adsorbent dose 2 g L^{-1} Temperature= 303K)

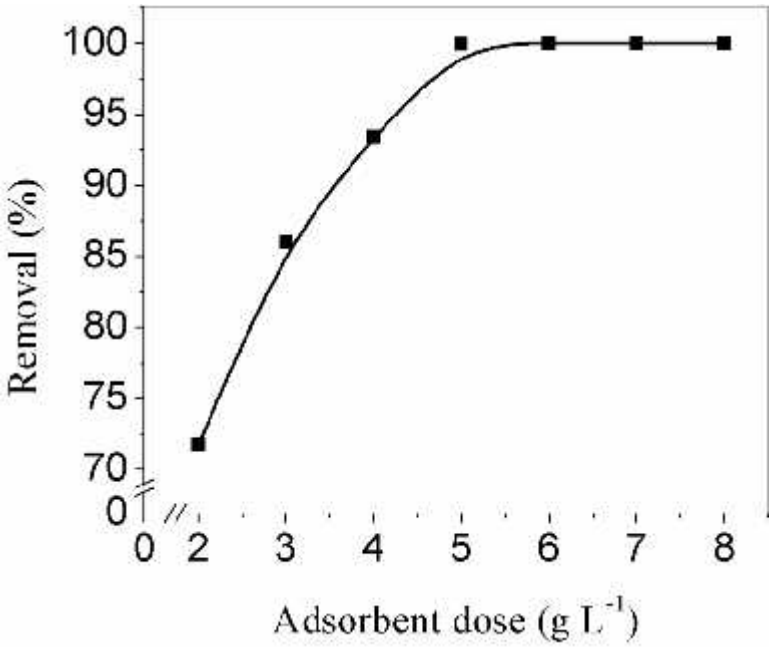

Figure 8.3 Effect of adsorbent dose on removal (%) of cadmium from aqueous solution on nano crystalline iron oxide/hydroxide (Initial pH=6, Initial concentration 20mg L^{-1}, Temperature 303K)

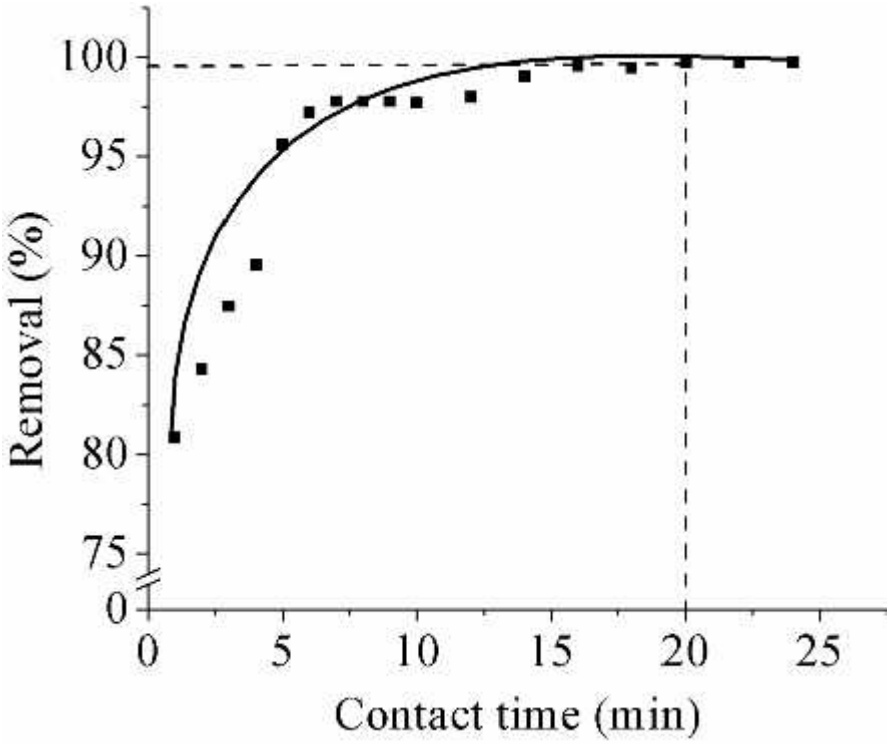

Figure 8.4 Effect of contact time on removal (%) of cadmium from aqueous solution on nano crystalline iron oxide/hydroxide (Initial concentration 20 mg L^{-1}, Initial pH =7, adsorbent dose 4g L^{-1}, Temperature= 303K)

8.1.1. Data analysis and construction of regression model

The regression analysis of the experimental data in BBD yielded the following regression equation for the removal (%) of cadmium using iron oxide/hydroxide:

$$Y = 82.67 - 13.48 \text{ (initial concentration)} + 2.15 \text{ (pH)} + 8.400 \text{ (adsorbent dose)} + 2.61 \text{ (initial concentration)}^2 - 1.0772 \text{ (pH)}^2 - 2.5344 \text{ (adsorbent dose)}^2 + 0.9144 \text{ (initial concentration x pH)} + 2.2769 \text{ (initial concentration x adsorbent dose)} + 0.2856 \text{ (pH x adsorbent dose)} \quad (8.1)$$

The empirical model in terms of actual parameters (uncoded) is written as follows:

$$Y = 84.90 - 2.39 \text{ (initial concentration)} + 4.708 \text{ (pH)} + 17.2465 \text{ (adsorbent dose)} + 0.01163 \text{ (initial concentration)}^2 - 0.478773 \text{ (pH)}^2 - 2.53438 \text{ (adsorbent dose)}^2 + 0.04063 \text{ (initial concentration x pH)} + 0.151792 \text{ (initial concentration x adsorbent dose)} + 0.190417 \text{ (pH x adsorbent dose)} \quad (8.2)$$

Table 8.1 Box-Behnken designed experimental runs for removal of cadmium utilizing nano crystalline iron oxide/hydroxide

Run order	Initial Conc. (mg L^{-1})	pH	Adsorbent dose (g L^{-1})	Removal (%)
1	20	4	2	86.45
2	50	4	2	57.74
3	20	7	2	93.65
4	50	7	2	60.22
5	20	4	4	100
6	50	4	4	72.02
7	20	7	4	99.97
8	50	7	4	84.02
9	20	5.5	3	99.36
10	50	5.5	3	70.60
11	35	4	3	81.34
12	35	7	3	81.23
13	35	5.5	2	66.80
14	35	5.5	4	92.86
15	35	5.5	3	83.46
16	35	5.5	3	82.63
17	35	5.5	3	82.80
18	35	5.5	3	82.97
19	35	5.5	3	82.63
20	35	5.5	3	82.80

8.1.2. Regression analysis and ANOVA

The R^2 square is 96.22% (Table 8.2), it predicts good fit of the model as it is more than 80% (Yuliwati *et al.* 2012).Hence regression model better explained the behaviour of cadmium on nano iron oxide/hydroxide (Sarkar and Majumdar 2011). The magnitude of coefficient to the variable estimates the strength of the variable. The sign afore to the coefficient predicts the character of the variable. The positive sign afore to the coefficient intent the cadmium removal (%) to be increased with increase in variable and *vice versa* (Sarkar and Majumdar 2011). On the basis of aforementioned facts, initial concentration was most efficacious variable. It was followed by adsorbent dose and pH. The initial concentration had

negative sign afore to its coefficient, hence cadmium removal (%) decreases on increase of initial concentration. So, maximum removal will be achieved at lower feasible initial concentration. The coefficient of pH and adsorbent dose has positive sign afore to itself, suggesting increased removal with increase in initial concentration.

Table 8.2 Estimated Regression Coefficients for removal of cadmium using iron oxide/ hydroxide

Term	Coef	SE Coef	p
Constant	82.6738	1.11	0
initial concentration	-13.4827	1.021	0
pH	2.1531	1.021	0.061
adsorbent dose	8.4002	1.021	0
initial concentration*initial concentration	2.6183	1.947	0.208
pH*pH	-1.0772	1.947	0.592
adsorbent dose*adsorbent dose	-2.5344	1.947	0.222
initial concentration*pH	0.9144	1.142	0.442
initial concentration*adsorbent dose	2.2769	1.142	0.074
pH*adsorbent dose	0.2856	1.142	0.807
S = 3.22866, PRESS = 1350.89			
R-Sq = 96.22% , R-Sq(pred) = 50.96 %, R-Sq(adj) = 92.81%			

ANOVA was also used to check model fitness and significance of the effect of variables. The p value of less than 0.05 suggested the model term to be significant. Only initial concentration and adsorbent dose were found to be significant. Adjusted sum of squares was largest for initial concentration and afterwards it has been followed by adsorbent dose and initial pH. Also, ANOVA predicted the initial concentration to be most dominating factor followed by adsorbent dose and initial pH.

Table 8.3 Analysis of Variance for removal of cadmium using iron oxide/hydroxide

Source	DF	Seq SS	Adj SS	Adj MS	F	p
Regression	9	2650.49	2650.49	294.5	28.25	0
Linear	3	2569.84	2569.84	856.61	82.18	0
initial concentration	1	1817.85	1817.85	1817.85	174.39	0
pH	1	46.36	46.36	46.36	4.45	0.061
adsorbent dose	1	705.64	705.64	705.64	67.69	0
Square	3	31.84	31.84	10.61	1.02	0.425
initial concentration*initial concentration	1	1.02	18.85	18.85	1.81	0.208
pH*pH	1	13.16	3.19	3.19	0.31	0.592
adsorbent dose*adsorbent dose	1	17.66	17.66	17.66	1.69	0.222
Interaction	3	48.81	48.81	16.27	1.56	0.259
initial concentration*pH	1	6.69	6.69	6.69	0.64	0.442
initial concentration*adsorbent dose	1	41.47	41.47	41.47	3.98	0.074
pH*adsorbent dose	1	0.65	0.65	0.65	0.06	0.807
Residual Error	10	104.24	104.24	10.42		
Lack-of-Fit	5	103.76	103.76	20.75	215.86	0
Pure Error	5	0.48	0.48	0.1		
Total	19	2754.73				
R-Sq = 96.22%	R-Sq(pred) = 50.96 %			R-Sq(adj) = 92.81%		

8.1.3. Effect of initial concentration

Initial concentration was the most dominating factor among all factors to be analysed in the study. The cadmium removal (%) decreased with rise of initial concentration. This can be easily seen by comparing experimental runs ‘1,2’ and ‘3,4’ (Table 8.1). There were limited numbers of active sites present on the surface of the adsorbent. Initially, large number of active site was available as compared to the adsorbate concentration. The unsaturated sites turned out to be saturated on increasing initial concentration; it leads to less number of unsaturated sites available for adsorption. Hence, cadmium removal (%) decreased on increasing the initial cadmium concentration.

8.1.4. Effect of pH

The pH has the least dominating effect on the removal (%) of cadmium among all variables to be studied. The trivial effect of pH can be seen by comparison of

Experimental runs '1;3' and '2;4' (Table 8.1). The removal (%) of cadmium declined on decreasing the pH of the solution. With a drop in the pH of the solution the surface charge of the adsorbent becomes more positive. Hence, electrostatic attraction declined between adsorbent and adsorbate, it leads to decrease in removal (%) of cadmium. In addition to aforementioned electrostatic effect on cadmium removal (%); the H^+ ions also compete with cadmium ions for adsorption on the surface of adsorbent (Wang *et al.* 2010). The decline in pH leads to increase in the number of H^+ ions. So, the competition between H^+ and cadmium ions becomes more intense; it leads to decrease in removal (%) of the cadmium.

8.1.5. Effect of adsorbent dose

The cadmium removal (%) increased on increasing the adsorbent dose (Experimental runs '1:5' and '2:6' in Table 8.1). The number of unsaturated active sites raised on increasing the adsorbent dose. The maximum amount of cadmium removal (%) was achieved at $4gL^{-1}$ (initial concentration 20 mg L^{-1} in Experimental run 5). Response surface plot (Figure 8.5) depicted highest amount of cadmium removal (%) at lower and upper ends of adsorbent dose with pH at 7. The hefty amount of active sites is the reason to this finding.

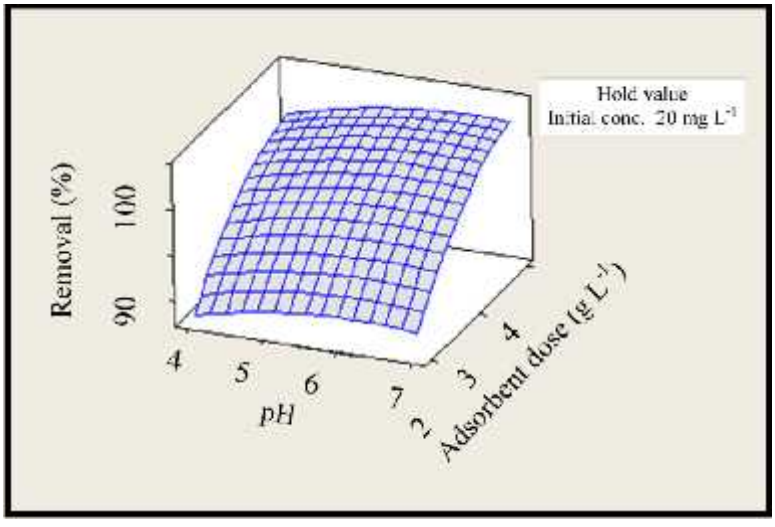

Figure 8.5 Surface plot of 'cadmium removal (%) *vs.* pH and adsorbent dose' at hold values of initial concentration at 20 mg L^{-1}

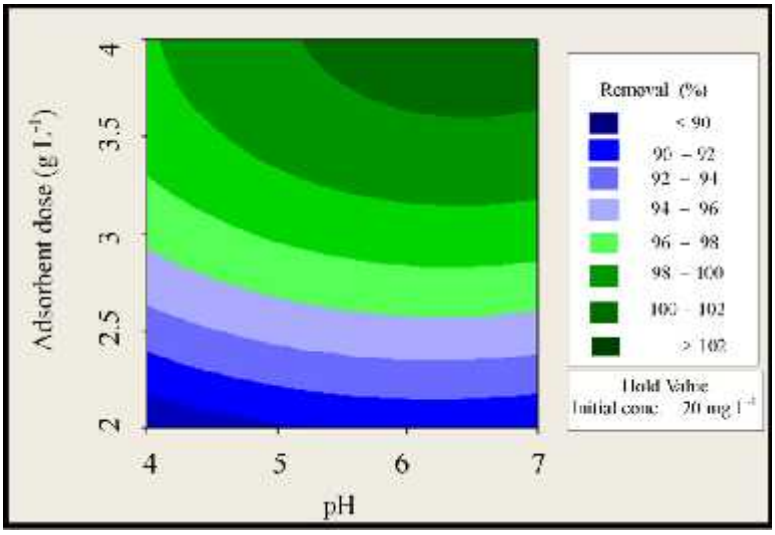

Figure 8.6 Contour plot of 'cadmium removal (%) *vs.* pH and adsorbent dose' at hold values of initial concentration at 20 mg L^{-1}

8.1.6. Response surface and contour plots

Response surface and contour plot (Figure 8.5 to 8.10) depicted that higher cadmium removal (%) was achieved at lower initial concentration and higher adsorbent dose. The Figure 8.6 shows that the pH has negligible effect up to the adsorbent dose of 3 g L^{-1}. After the adsorbent dose of 3.5 to 4 g L^{-1} the removal increased with increase of pH. The Figures 8.7 and 8.8 depict increased removal (%) with decrease in initial concentration and increase of adsorbent dose.

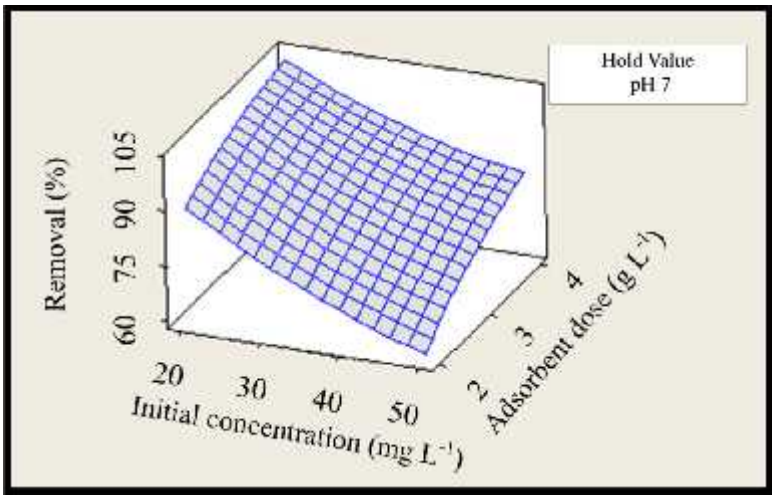

Figure 8.7 Surface plot of 'cadmium removal (%) *vs.* adsorbent dose and initial concentration' at hold value of pH at 7

At pH 7, the cadmium removal (%) was more than 60 predicted at all range of other conditions in the model (Figures 8.7 and 8.8). In addition to this, more than ca. 90 % cadmium removal is achieved at initial concentration 20 mg L^{-1} at all conditions (Figure 8.6) except at pH lower than 5. In the range of pH 6 to 7 cadmium removal (%) of more than ca. 80 is predicted at hold value of adsorbent dose 4 g L^{-1} (Figure 8.9).

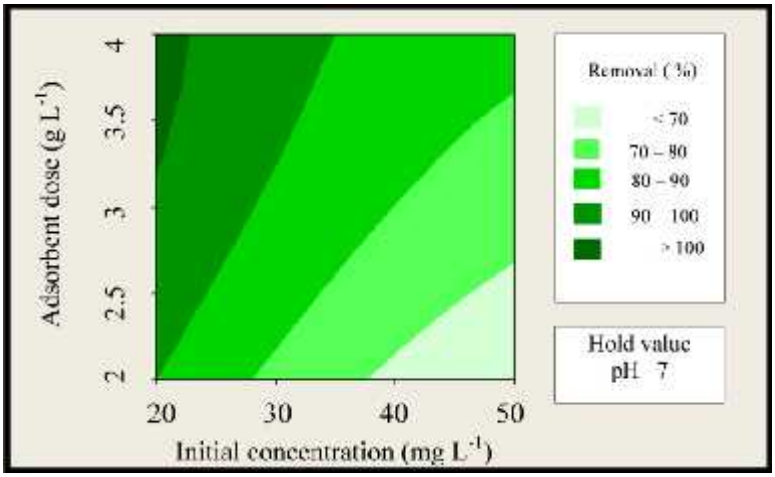

Figure 8.8 Contour plot of 'cadmium removal (%) *vs.* adsorbent dose and initial concentration' at hold value of pH at 7

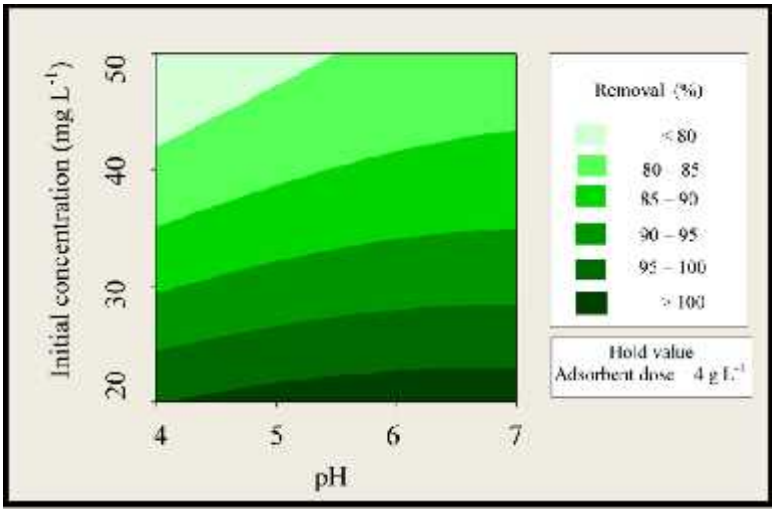

Figure 8.9 Contour plot of 'cadmium removal (%) *vs.* pH and initial concentration' at hold values of adsorbent dose at 4 g L^{-1}

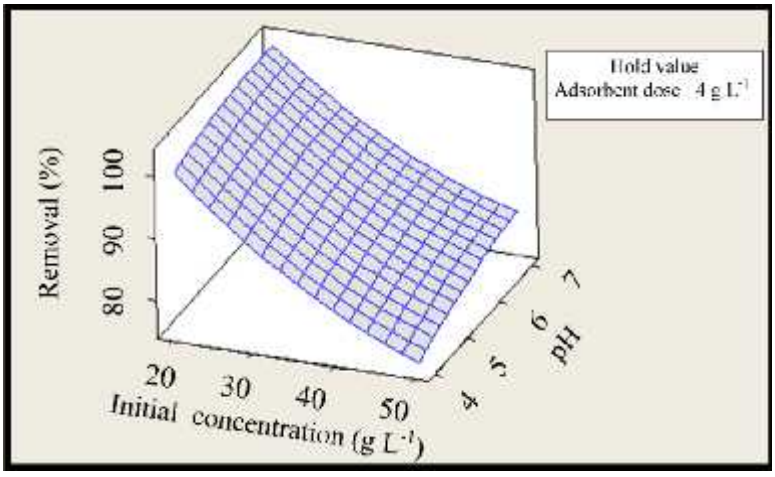

Figure 8.10 Surface plot of 'cadmium removal (%) *vs.* pH and initial concentration' at hold values of adsorbent dose at 4 g L^{-1}

8.1.7. Confirmation experiments

Optimized result suggested by Minitab 16 software on the basis RSM experimental results is presented in Figure 8.11. The optimized results were as follows: initial pH = 6.4, Initial concentration of cadmium = 23.62 mg L^{-1} and adsorbent dose = 3.8 g L^{-1}.

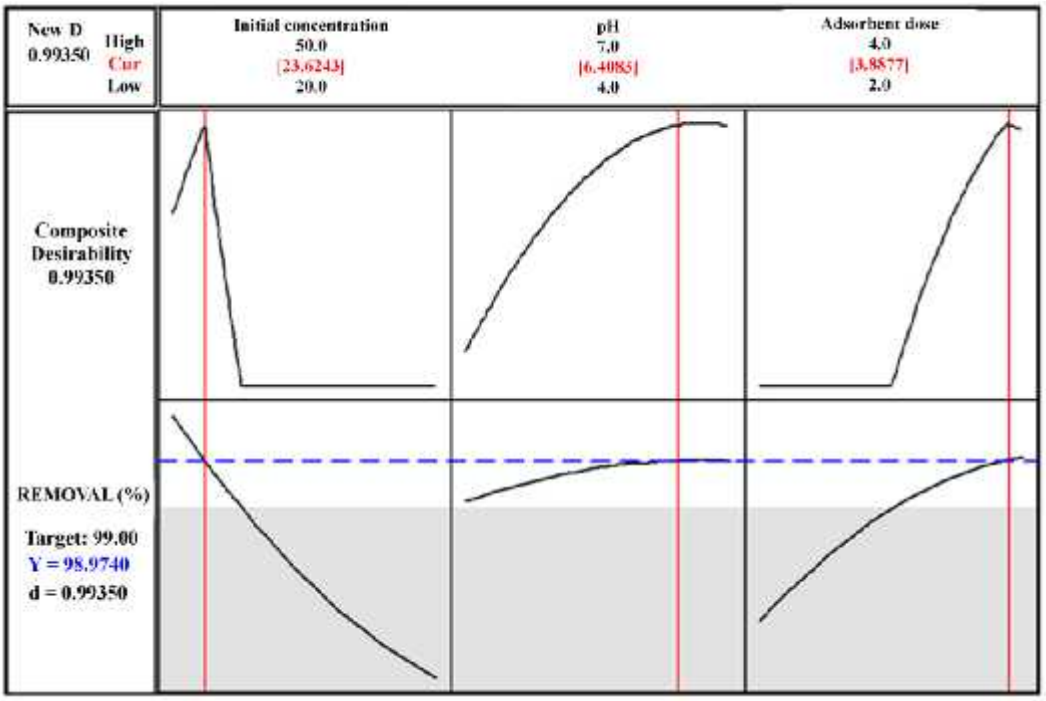

Figure 8.11 Optimization plot of removal of cadmium with iron oxide/hydroxide

The verification of predicted adsorption results was conducted at varying conditions (Table 8.4). The results closely matched with the predicted results but

only at higher pH. It suggested the model is able to predict the data only at higher pH. However, even at higher pH with lower adsorbent dose (2 g L^{-1}), the variations between experimental and theoretical results were extensive (Table 8.4).

Table 8.4 Confirmation experiments for removal of cadmium using nano crystalline iron oxide/hydroxide

S.No.	Initial conc. (mg L^{-1})	pH	Adsorbent dose (g L^{-1})	Experimental values	Predicted values
1	50	6	5	87	84.11*
2	22	6	6	100	93.41*
3	30	4	6	100	83.79*
4	42	7	4	85.83	85.66
5	48	4	6	92.47	76.38*
6	27	6	4	99.88	95.79
7	27	6.5	4	99.81	96.08
8	25	5	4	99.86	96.44
9	23	6	4	100	99.62
10	23	6.5	4	99.93	99.83
11	50	6	2	44	59.40
12	22	6	2	69.81	87.60
13	30	4	2	43.43	74.64
14	42	7	2	47.50	66.17
15	48	4	2	32.25	56.31

*Samples were outside the model data

Table 8.5 Optimization experiments for removal of cadmium using nano crystalline iron oxide/hydroxide

S.No.	Initial conc. (mg L^{-1})	pH	Adsorbent dose (g L^{-1})	Removal (%)
1	23	6.4	4	99.68
2	22	7	4	100
3	23	7	4	100
4	24	7	4	100
5	25	7	4	100
6	26	7	4	100
7	27	7	4	100
8	28	7	4	99.74
9	29	7	4	99.75
10	30	7	4	99.29
11	27	7	3.5	98.20
12	27	7	3	83.30
13	27	7	2.5	75.92
14	27	7	2	74.07

The optimization obtained by Minitab 16 software, RSM model is further optimized by variation of pH, adsorbent dose and initial concentration one by one

(Table 8.5).The optimization of results lead to following conditions: initial concentration 27 mg L^{-1}, pH =7 and adsorbent dose of 4 g L^{-1}.

8.2. Linear approach for isotherm analysis

The linear Langmuir isotherm plot (Figure 8.12) showed the predicted data is closely proximate to experimental data. The linear Freundlich isotherm plot (Figure 8.13) depicts that experimental data is less proximate to the predicted data. The plots (Figures 8.12 and 8.13) clearly distinguished the suitability of Langmuir isotherm model to experimental data.

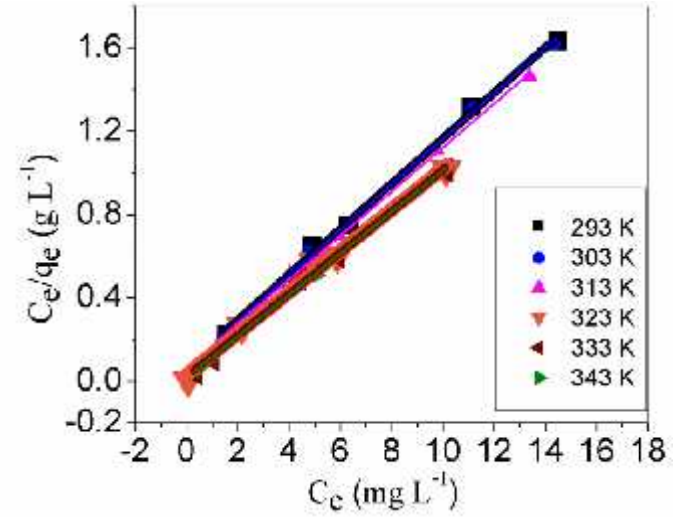

Figure 8.12 Linear Langmuir isotherm plot of cadmium removal using nano crystalline iron oxide/hydroxide (dots represent the experimental data and lines represent the data estimated by the model)

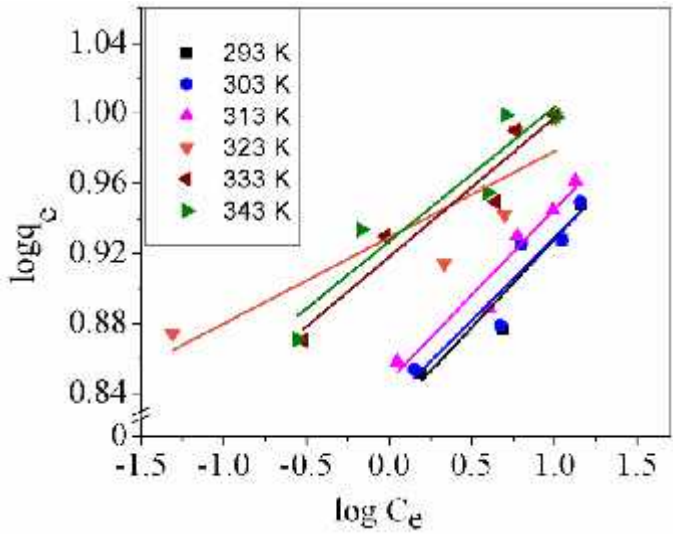

Figure 8.13 Linear Freundlich isotherm plot of cadmium removal using nano crystalline iron oxide/hydroxide (dots represent the experimental data and lines represent the data estimated by the model)

The isotherm parameters determined by linear analysis (Figures 8.12 and 8.13) are presented in Table 8.6. The Langmuir constants Q_o and b were obtained from the slope and intercept of 'C_e/q_e *vs.* C_e' plot respectively. The value of Q_o increased with temperature, depicting increase in maximum adsorption capacity with increase of temperature. Similarly, Freundlich isotherm parameters K_F and 1/n were calculated from the intercept and slope of plot 'log q_e *vs.* log C_e' respectively. Coefficient of determination was superior for Langmuir isotherm as compared to Freundlich isotherm. Hence, adsorption of cadmium by iron oxide/hydroxide is better explained by Langmuir isotherm as compared to Freundlich isotherm on the basis of coefficient of determination (R^2_{adj}).

Table 8.6 Langmuir and Freundlich isotherm parameters along with coefficient of determination for linear analysis and nonlinear analysis by Microcal origin for adsorption of cadmium from aqueous solution on nano crystalline iron oxide/hydroxide

		Langmuir parameters			**Freundlich parameters**		
	Temp. (K)	**Q_o (mg/g)**	**b (L/mg)**	**R^2_{adj}**	**K_F (mg/g)(L/mg)$^{1/n}$**	**1/n**	**R^2_{adj}**
Linear	293	9.1785	1.4153	0.9960	6.7255	0.1003	0.8394
	303	9.1591	1.5272	0.9961	6.8364	0.0943	0.8520
	313	9.4652	1.6124	0.9972	7.0355	0.0978	0.9240
	323	10.109	3.0596	0.9916	8.4963	0.0491	0.6976
	333	10.095	4.2202	0.9967	8.2809	0.0794	0.9088
	343	10.070	5.8966	0.9977	8.4520	0.0766	0.8508
Microcal origin	293	8.8197	2.3553	0.6935	0.3060	0.0223	0.8386
	303	8.7789	2.7400	0.6844	0.2783	0.0201	0.8513
	313	8.9919	3.2020	0.7151	0.1940	0.0142	0.9279
	323	9.2077	87.447	0.3834	0.2962	0.0178	0.6822
	333	9.6695	10.095	0.8075	0.1806	0.0133	0.9029
	343	9.8130	10.781	0.8520	0.2225	0.0163	0.8439

8.3. Nonlinear approach for isotherm analysis

Nonlinear analysis was performed by error analysis using solver add-in of Microsoft excel (Figures 8.14 and 8.15) and customized curve fitting function of

Microcal origin (Figures 8.16 and 8.17). The nonlinear Freundlich isotherm plot (Figure 8.14) depicts the vast difference between the experimental data and data predicted by error analysis method.

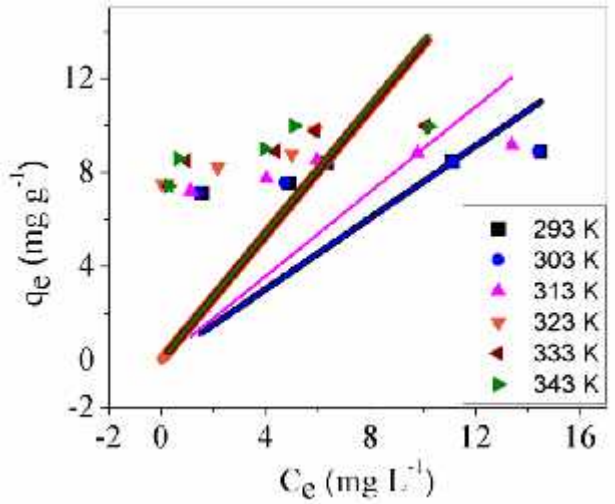

Figure 8.14 Nonlinear Freundlich isotherm plot of cadmium removal using nano crystalline iron oxide/hydroxide obtained by error analysis method (dots represent the experimental data and lines represent the data estimated by the model)

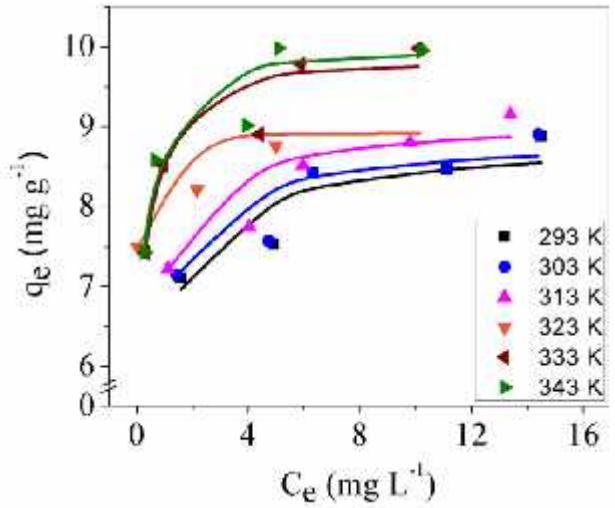

Figure 8.15 Nonlinear Langmuir isotherm plot of cadmium removal using nano crystalline iron oxide/hydroxide obtained by error analysis method (dots represent the experimental data and lines represent the data estimated by the model)

The data predicted by error analysis method depicted in Langmuir isotherm plot (Figure 8.16) is closer to experimental data than in Freundlich isotherm plot (Figure 8.14). However, the data predicted by error analysis method in Langmuir isotherm plot (Figure 8.15) is also less proximate to experimental data than in

linear analysis method (Figure 8.12). The estimated isotherm parameters by nonlinear analysis are presented in Tables 8.6 and 8.7. In error analysis method, the isotherm with minimum normalized sum of error function is selected as optimum error function. The optimum error function is used for parameter determination. Error function analysis of Langmuir isotherm resulted in three, two and one systems to be better explained by ARE, EABS and HYBRID respectively. Similarly in error analysis of Freundlich isotherm; three systems are well explained by HYBRID, two systems are better explained by MPSD and one system by ARE. The coefficient of determination was higher for Langmuir isotherm (Table 8.7). It suggested the appropriateness of Langmuir isotherm model for present system. Nonlinear analysis was also performed using customized curve fitting function of Microcal origin. The nonlinear Langmuir isotherm plot (Figure 8.16) depicts the less proximity between the experimental data and data predicted by customized Microcal origin function.

Table 8.7 Langmuir, Freundlich isotherm parameters along with coefficient of determination by error analysis method for adsorption of cadmium from aqueous solution on nano crystalline iron oxide/hydroxide

	Langmuir parameters				**Freundlich parameters**			
Temp. (K)		**Q_o (mg/g)**	**b (L/mg)**	**R^2_{adj}**		**K_F $(mg/g)(L/mg)^{1/n}$**	**1/n**	**R^2_{adj}**
293	HYBRID	8.7886	2.4184	0.5389	MPSD	0.8777	0.8666	-61.10
303	ARE	8.8381	2.9587	0.4757	MPSD	0.8917	0.8530	-66.21
313	EABS	9.0628	3.4794	0.5159	ARE	0.8999	1.00	-58.05
323	ARE	8.9212	106.86	-0.069	HYBRID	1.3448	1.00	-46.67
333	ARE	9.8506	10.074	0.6462	HYBRID	1.3478	1.00	-58.74
343	EABS	9.9890	10.327	0.7351	HYBRID	1.3604	1.00	-64.13

The data predicted by customized Microcal origin function depicted in Freundlich isotherm plot (Figure 8.17) is also less proximate to experimental data. However, experimental data at locations in Freundlich isotherm plot (Figure 8.17) are slightly more proximate to predicted data than in Langmuir isotherm plot (Figure 8.16). This predicts the suitability of Freundlich isotherm plot for explanation of isotherm data.

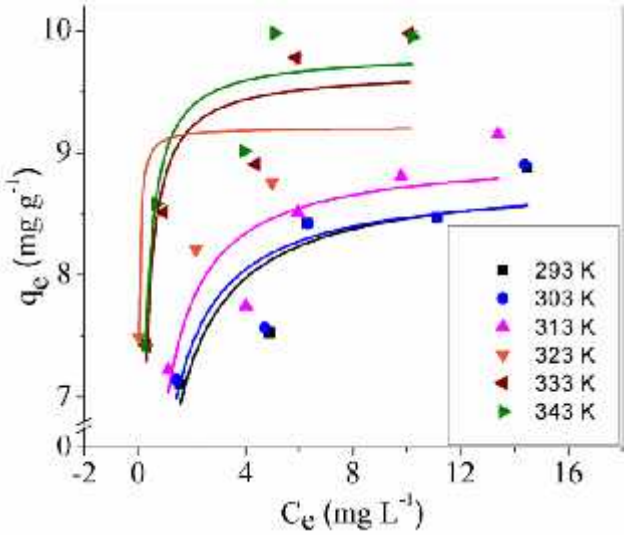

Figure 8.16 Nonlinear Langmuir isotherm plot of cadmium removal using nano crystalline iron oxide/hydroxide obtained by customized Microcal origin function (dots represent the experimental data and lines represent the data estimated by the model)

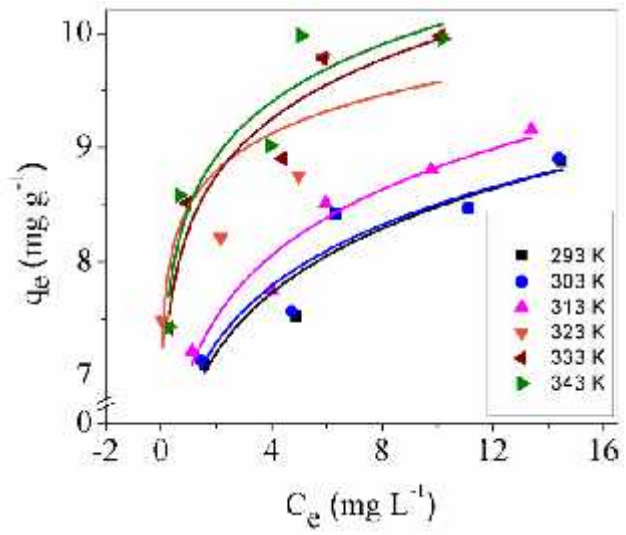

Figure 8.17 Nonlinear Freundlich isotherm plot of cadmium removal using nano crystalline iron oxide/hydroxide obtained by customized Microcal origin function (dots represent the experimental data and lines represent the data estimated by the model

The coefficient of determination by customized Microcal origin function for Langmuir isotherm model was lower than Freundlich isotherm model (Table 8.6). Hence, it also predicts the suitability of Freundlich isotherm model. The coefficient of determination values was highest for linear analysis. So, linear analysis is preferred over nonlinear analysis (curve fitting using Microcal origin and curve fitting using error analysis) due to high coefficient of determination.

8.4. Linear approach for kinetic model analysis

The linear pseudo-first order plot (Figure 8.18) showed the predicted data is less proximate at to experimental data points. The linear pseudo-second order plot (Figure 8.19) depicts the close proximity of experimental and predicted data. This predicts the suitability of pseudo-second order kinetic model for explanation of kinetic data.

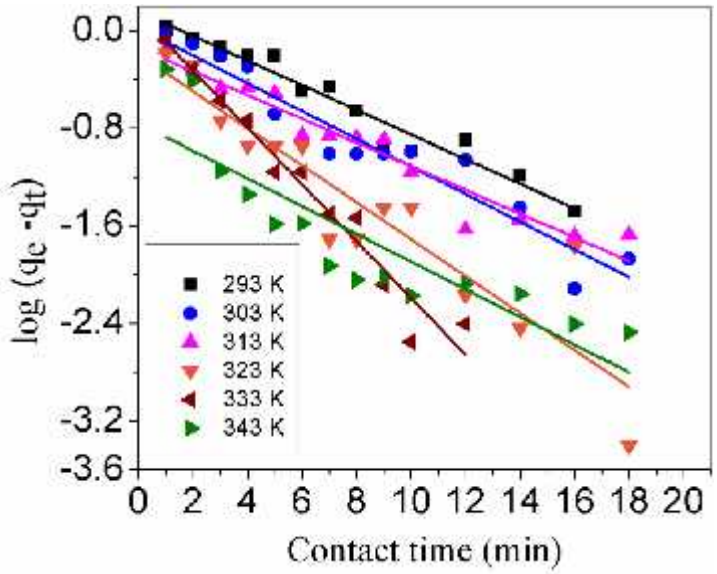

Figure 8.18 Linear pseudo-first order plot of cadmium removal using nano crystalline iron oxide/hydroxide (dots represent the experimental data and lines represent the data estimated by the model)

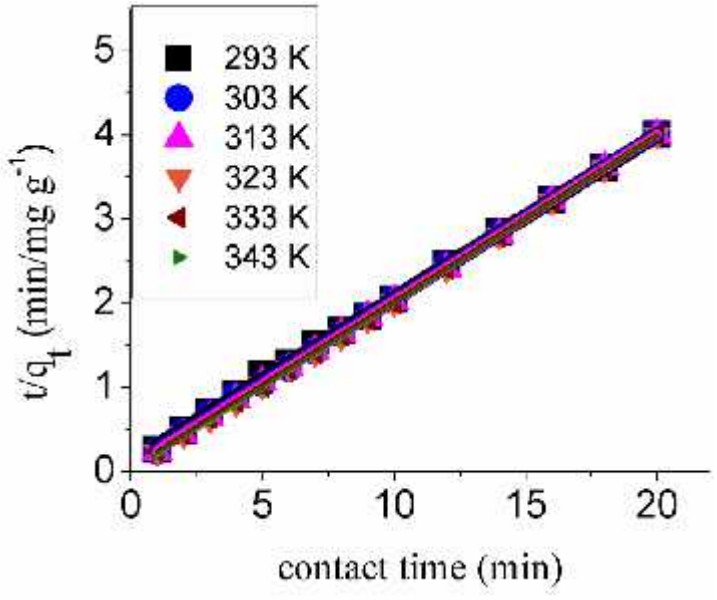

Figure 8.19 Linear pseudo-second order plot of cadmium removal using nano crystalline iron oxide/hydroxide (dots represent the experimental data and lines represent the data estimated by the model)

The parameters along with their coefficient of determination (R^2_{adj}).obtained from linear analysis (Figures 8.18 and 8.19) of kinetic data are represented in Table 8.8. The coefficient of determination (R^2_{adj}) suggests pseudo-second order model fits better as compared to pseudo-first order model. The theoretical q_e values retrieved from pseudo-second order model were closer to experimental values as compared to theoretical q_e values computed from pseudo-first order model.

Table 8.8 Pseudo-first order and pseudo-second order kinetic parameters for linear analysis for adsorption of cadmium from aqueous solution on nano crystalline iron oxide/hydroxide

			Pseudo-first order			Pseudo-second order		
	Temp. (K)	Experimental q_e (mg/g)	q_e (mg/g)	k_1 (min^{-1})	R^2_{adj}	q_e (mg/g)	k_2 ($g/mg^{-1} min^{-1}$)	R^2_{adj}
Linear	293	4.74	1.4384	0.2322	0.9482	5.1295	0.3421	0.9996
	303	4.98	1.0532	0.2612	0.9095	5.0704	0.5564	0.9998
	313	4.85	0.7258	0.2236	0.9346	5.0599	0.7150	0.9999
	323	4.99	0.6361	0.3483	0.8337	5.0329	1.3613	0.9999
	333	4.98	1.3705	0.5359	0.9550	5.0339	1.2980	0.9999
	343	4.96	0.1745	0.2611	0.7572	5.0193	2.7205	0.9999

8.5. Nonlinear approach for kinetic model analysis

The nonlinear pseudo-first order plot (Figure 8.20) depicts the proximity between the experimental data and data predicted by error analysis method except at few points.

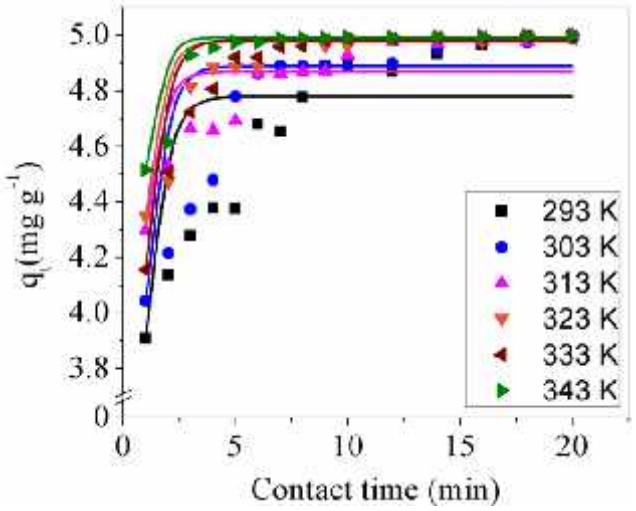

Figure 8.20 Nonlinear pseudo-first order plot of cadmium removal using nano crystalline iron oxide/hydroxide obtained by error analysis function (dots represent the experimental data and lines represent the data estimated by the model)

Similarly, nonlinear pseudo-second order plot (Figure 8.21) also depicts the close proximity between the experimental data and data predicted by error analysis method except at few points. The two plots (Figures 8.20 and 8.21) cannot be able to differentiate the suitability of the preferred kinetic model.

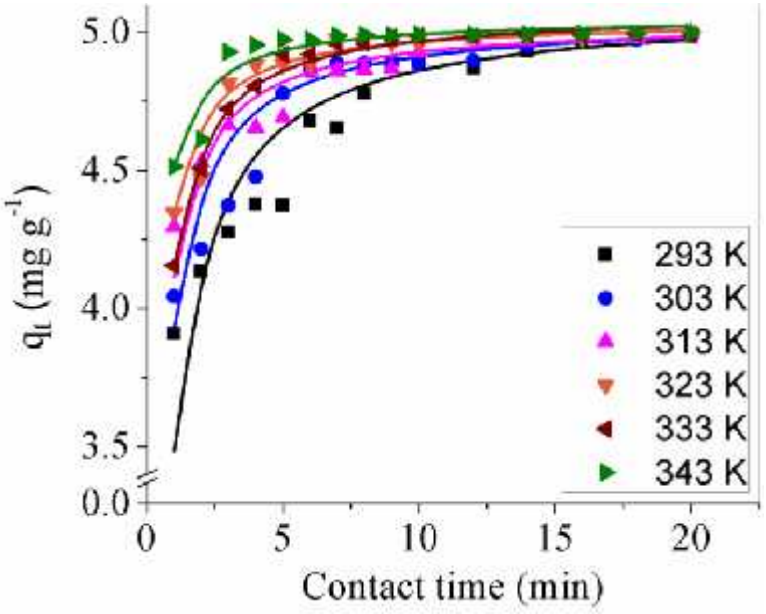

Figure 8.21 Nonlinear pseudo-second order plot of cadmium removal using nano crystalline iron oxide/hydroxide obtained by error analysis function (dots represent the experimental data and lines represent the data estimated by the model)

Kinetic model parameters determined via nonlinear method (Figure 8.20 to 8.23) are revealed in Tables 8.9 and 8.10.In error analysis method, the error function with least normalized sum is selected. In pseudo-first order model; out of six systems, three systems are explained by ARE; two systems are explained by EABS. One system has least normalized sum of error for MPSD. Similarly in pseudo-second order model, three systems each have least normalized sum for ARE and EABS. The theoretical q_e values were much closer to experimental values in pseudo-second order model as compared to pseudo-first order model. Pseudo-second order model was preferred to be a better model as compared to pseudo-first order model for the present system on the basis of coefficient of determination as compared to Pseudo-first order model.

Table 8.9 Pseudo-first order and pseudo-second order model constants by error analysis method for adsorption of cadmium from aqueous solution on nano iron oxide/hydroxide

	Pseudo-first order				Pseudo-second order			
Temp. (K)	**Error function**	**k_1 min^{-1}**	**q_e (mg/g)**	**R^2_{adj}**	**Error function**	**k_2 (g/mg^{-1} min^{-1})**	**q_e**	**R^2_{adj}**
293	ARE	1.7024	4.7783	0.3239	EABS	0.4270	5.0868	0.9908
303	MPSD	1.7492	4.8883	0.3566	EABS	0.6912	5.0527	0.9952
313	ARE	2.1415	4.8672	0.4824	ARE	0.8801	5.0399	0.9981
323	EABS	2.0698	4.9754	0.5081	EABS	1.2354	5.0450	0.9987
333	EABS	1.7975	4.9814	0.6914	ARE	0.8873	5.0782	0.9996
343	ARE	2.3494	4.9909	0.5682	ARE	1.6609	5.0528	0.9990

Table 8.10 Pseudo-first order and pseudo-second order kinetic parameters for nonlinear analysis by Microcal origin for adsorption of cadmium from aqueous solution on nano crystalline iron oxide/hydroxide

			Pseudo-first order			Pseudo-second order		
	Temp. (K)	**Experimental q_e (mg/g)**	**q_e (mg/g)**	**k_1 (min^{-1})**	**R^2_{adj}**	**q_e (mg/g)**	**k_2 (g/mg^{-1} min^{-1})**	**R^2_{adj}**
Microcal origin	293	4.74	4.7762	1.4272	0.4350	5.0078	0.5301	0.8423
	303	4.98	4.8455	1.5266	0.5116	5.0371	0.6424	0.8853
	313	4.85	4.8754	1.9956	0.5279	5.0034	1.0464	0.9088
	323	4.99	4.9354	1.9564	0.6423	5.0506	1.1190	0.9239
	333	4.98	4.9376	1.7024	0.7904	5.0757	0.8840	0.9794
	343	4.96	4.9690	2.2603	0.6559	5.0513	1.6004	0.8797

The nonlinear pseudo-first order plot (Figure 8.22) and pseudo-second order plot (Figure 8.23) showed proximity of experimental data and data predicted by customized Microcal origin function. The two plots (Figures 8.22 and 8.23) cannot be able to differentiate the suitability of the better model. Kinetic data analysis with Microcal origin curve fitting function suggested pseudo-second order model on the basis of high coefficient of determination to be better for present model (Table 8.10). Pseudo-second order model succeeded in fitting the kinetic data much better by linear analysis and nonlinear analysis. There is not any distinction between error analysis method and curve fitting analysis via Microcal origin in suggesting the pseudo-second order model as preferable model for fitting kinetic data. The linear analysis method prevailed over nonlinear analysis method for determination of kinetic parameters due to high R^2_{adj} .

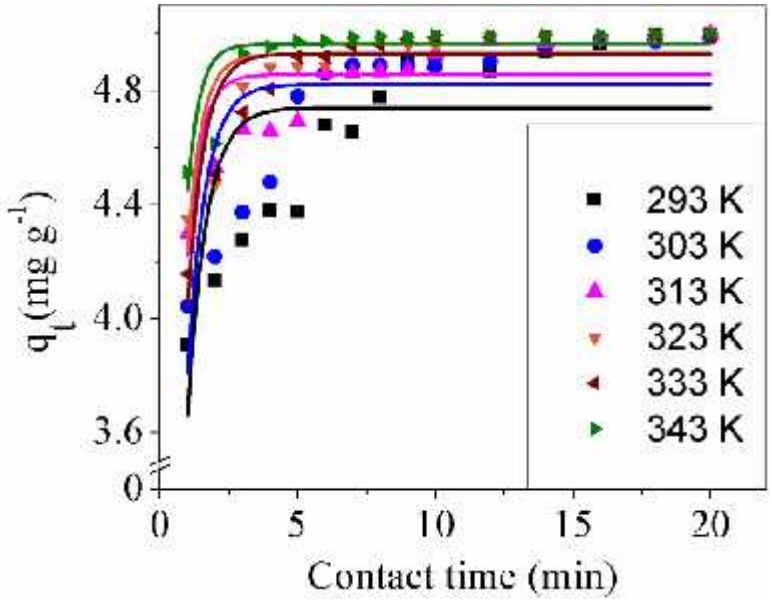

Figure 8.22 Nonlinear pseudo-first order plot of cadmium removal using nano crystalline iron oxide/hydroxide obtained by customized Microcal origin function (dots represent the experimental data and lines represent the data estimated by the model)

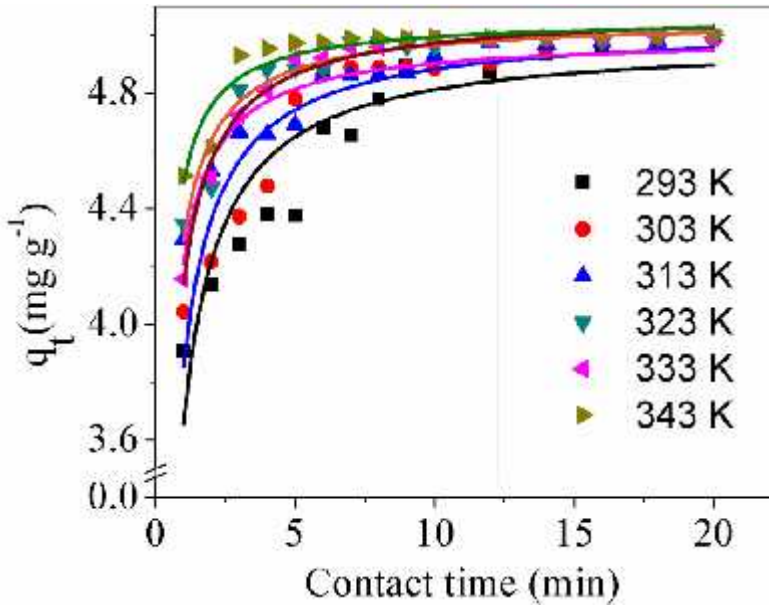

Figure 8.23 Nonlinear pseudo-second order plot of cadmium removal using nano crystalline iron oxide/hydroxide obtained by customized Microcal origin function (dots represent the experimental data and lines represent the data estimated by the model)

8.6. Intraparticle diffusion model

The kinetics data was fitted in intraparticle diffusion model suggested by Weber and Morris (Weber and Morris 1963). Intraparticle diffusion graph plotted between q_t and $t^{1/2}$ is shown in Figure 8.24. The K_{diff}, C_b and R^2_{adj} are shown in Table 8.11. The intercept (C_b) depicts the thickness of boundary layer. The bigger

the value of intercept, bigger is the boundary layer. There were two regions in intraparticle diffusion plots. It depicts time dependent adsorption process.

Table 8.11 Intra particle diffusion model parameters for removal of cadmium using nano crystalline iron oxide/hydroxide

S.No.	Temperature (K)	K_{diff} (mg/g $min^{1/2}$)	C_b (mg g^{-1})	R^2_{adj}
1	293	0.3170	3.7527	0.8866
2	303	0.2580	4.0098	0.7549
3	313	0.1783	4.3042	0.8309
4	323	0.1500	4.4496	0.5981
5	333	0.1789	4.3523	0.5920
6	343	0.1019	4.6386	0.4652

Initially, the rate of cadmium uptake was faster and afterwards it slowed down with time. The regions marked as i and ii symbolize as domination of film diffusion and intraparticle diffusion respectively (Cheung *et al.* 2007). The intraparticle diffusion plot is not linear and does not pass through the origin. The slopes of first and second level show deviation from origin. The deviation of slope from origin is attributed to the difference in the mass transfer rate of initial and final stages of adsorption. It validates the existence of boundary layer diffusion as rate limiting mechanism for adsorption (Mohanty *et al.* 2005).

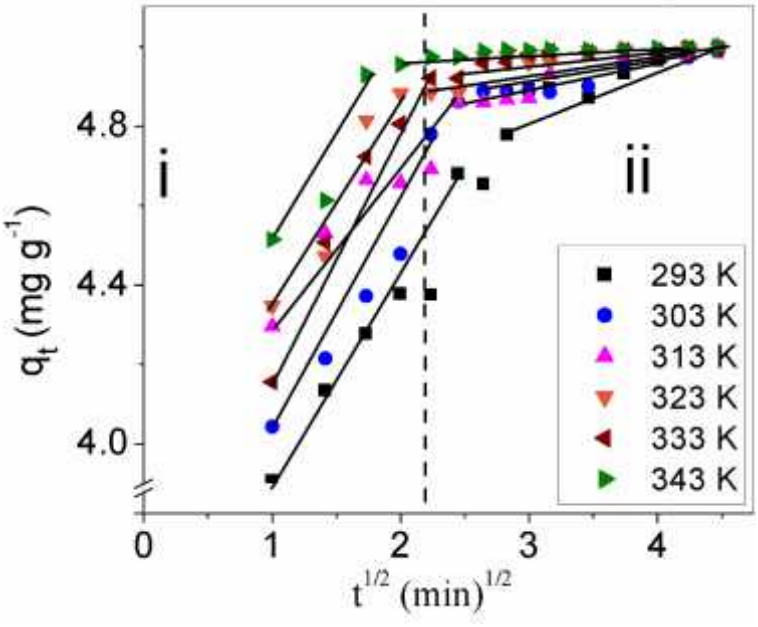

Figure 8.24 Intraparticle diffusion plot for adsorption of cadmium using nanocrystalline iron oxide/hydroxide

To further investigate the actual slow step of adsorption process; kinetic data is further analyzed with Boyd model simplified by Reichenberg (Boyd *et al.* 1947;Reichenberg 1953). Boyd model differentiates adsorption rate controlling step between boundary layer and particle diffusion (diffusion inside the pores). Boyd plot is represented by graph (Figure 8.25) between Bt *vs.* t. In the present case, graph (Figure 8.25) did not pass from the origin which means that the process of removal is not controlled by adsorption only, it administrated by boundary layer diffusion mechanism also.

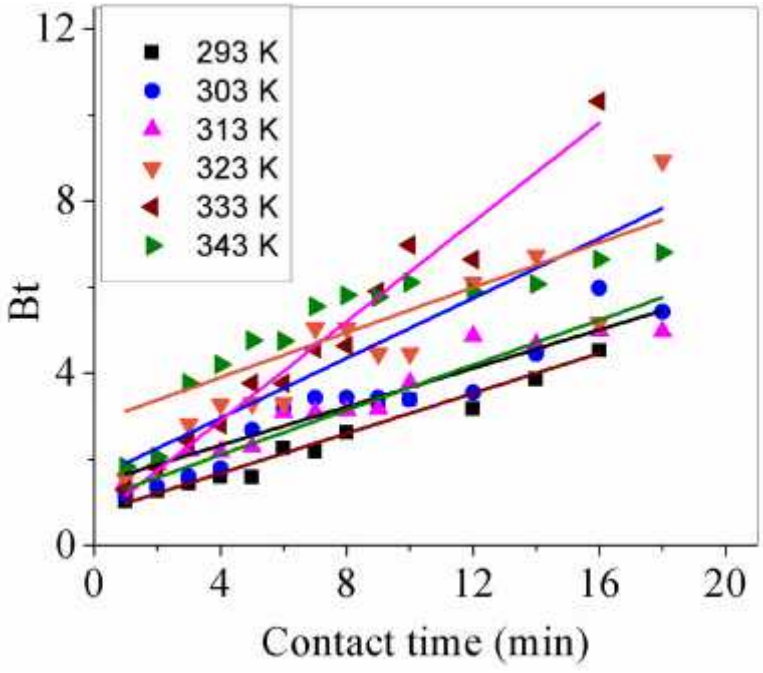

Figure 8.25 Boyd plot for adsorption of cadmium using nanocrystalline iron oxide/ hydroxide

8.7. Adsorption thermodynamics

8.7.1. Determination of thermodynamic parameters using Langmuir constant method

Thermodynamic parameters viz.. change in standard free energy (ΔG^o), change in standard enthalpy (ΔH^o) and change in standard entropy (ΔS^o) were estimated using subsequent equations (Gupta and Rastogi 2009;Liu 2009;Salvestrini *et al.* 2014):

$$\Delta G_e = -RT\ln K_L \quad (8.3)$$

$$\ln K_L = \frac{\Delta S_e}{R} - \frac{\Delta H_e}{RT} \quad (8.4)$$

The K_L is estimated from the following equation:

$$K_L = \frac{b}{\gamma_e} \quad (8.5)$$

$$\log\gamma_e = -A_1 z^2 I_e^{1/2} \quad (8.6)$$

Here, K_L (L mol^{-1}) is thermodynamic equilibrium constant calculated from the Langmuir constant b (Liu 2009), R is universal gas constant (8.314 J $mol^{-1}K^{-1}$), T is the temperature, γ_e is the activity coefficient, I_e is the ionic strength (8.89 x 10^{-5} mol/kg) of the solute at equilibrium, A_1 is a constant (0.509 $mol^{-1/2}$ $kg^{1/2}$) and z is the charge on ion.

Table 8.12 Thermodynamic parameters estimated by Langmuir constant method for adsorption of cadmium by nano crystalline iron oxide/hydroxide

Parameter	**Equation**	**Temp. (K)**	**Parameters using linear equation parameter b**	**Parameters using nonlinear equation parameter b (Microcal origin)**	**Parameters using nonlinear equation parameter b (excel)**
ΔG^o (kJ mol^{-1})	$\Delta G^o = -RT\ln K_L$	293	-27.582	-28.822	-28.8888
		303	-28.715	-30.187	-30.3822
		313	-29.804	-31.589	-31.806
		323	-32.476	-41.481	-42.0184
		333	-34.372	-36.786	-36.780
		343	-36.358	-38.079	-37.9572
ΔH^o (kJ mol^{-1})	$\ln K_L = \frac{\Delta S^0}{R} - \frac{\Delta H^0}{RT}$		25.57	36.288 (28.834*)	35.291 (27.325*)
ΔS^o (kJ $mol^{-1}K^{-1}$)			0.1796	0.2225 (0.1953*)	0.219 (0.1908*)
	R^2_{adj}		0.8825	0.1920 (0.9060*)	0.1421 (0.9213*)

*Except taking point of ln K_L at 323 K

The ΔH^o and ΔS^o were calculated from the slope and intercept of plot between $\ln K_L$ and 1/T respectively (Elkady *et al.* 2011). The calculated values ΔG^o, ΔH^o and ΔS^o parameters are presented in the Table 8.12.

Thermodynamic parameters were determined from nonlinear and linear analysis using Langmuir constant method i.e. b displays variation in magnitude. Both analysis advocated adsorption was spontaneous, endothermic and occurred with increase in entropy. The linear method is used as it has higher coefficient of determination (Table 8.7). Hence, this method is used to determine isotherm parameters. The positive value of change in enthalpy (25.57 kJ mol^{-1}) advocated the endothermic nature of the adsorption process. The negative values of ΔG^o predicted that the process to be spontaneous in nature. The value of ΔG^o decreases with rise of temperature. This shows the process becomes more feasible at higher temperature. The entropy change is positive (0.1796 kJ mol^{-1}). It demonstrates that adsorption of cadmium on nano iron oxide/hydroxide occurred with increase in entropy.

8.7.2. Determination of thermodynamic parameters using partition method

Partition method is also used in addition to Langmuir constant method for determination of thermodynamic parameters (Liu 2009;Salvestrini *et al.* 2014). Here, K_p or K_c is used in place of K_L:

$$K_P \text{ or } K_C = \frac{C_s}{C_w} \tag{8.7}$$

Here, C_s and C_w correspond to the concentration of adsorbate in solid and liquid media. Following determination of K_p, Equations 8.3 and 8.4 were employed for determination of thermodynamic parameters. Furthermore, change in free energy is also computed from the subsequent equations (Salvestrini *et al.* 2014):

$$\Delta G^o = \Delta H^o - T\Delta S^o \tag{8.8}$$

Table 8.13 Thermodynamic parameters calculated by partitioned method for adsorption of cadmium by nano crystalline iron oxide/hydroxide

Temp. (K)	**ΔG^o (kJ mol^{-1})**	**ΔH^o (kJ mol^{-1})**	**ΔS^o (kJ mol^{-1}K^{-1})**		**ΔG^o (kJ mol^{-1})**
	$\Delta G^o = -RT\ln K_L$	$\ln K_L = \frac{\Delta S^o}{R} - \frac{\Delta H^o}{RT}$		R^2_{adj}	$\Delta G^o = \Delta H^o - T\Delta S^o$
293	-18.514	-15.856	0.0073	-0.06198	-18.006
303	-14.920				-18.079
313	-21.531				-18.152
323	-18.984				-18.226
333	-17.193				-18.299
343	-17.986				-18.373

The thermodynamic parameters estimated by partition method are displayed in Table 8.13. The negative sign afore to the coefficient of change in enthalpy (ΔH^o = -15.856 kJ mol^{-1}), suggested exothermic nature of adsorption. The spontaneous nature of the process is validated by negative values of the ΔG^o. The ΔG^o values calculated from equation 8.8 were approximately similar and close to ca. -18 kJ mol^{-1}. The positive values of ΔS^o pointed to the augmentation of disorderness at adsorbate-adsorbent interface for the duration of adsorption of cadmium on iron oxide/hydroxide.

Both partition and Langmuir constant methods suggested that the system is spontaneous in nature and occurred with increase in entropy. Langmuir constant method recommended the process to be endothermic in nature, whereas the partition method suggested the process to be exothermic in nature. The values of Q_o (Langmuir constant) increased with temperature; it suggested that the adsorption capacity ascends with rise of temperature. The rise of Q_o supports the endothermic nature of adsorption. Hence, Langmuir constant method is employed for determination of change in enthalpy. The K_c is equal to the thermodynamic equilibrium constant (K_L) only at dilute concentration (Liu 2009). So, all other thermodynamic parameters were also calculated using Langmuir constant method.

8.7.3. Activation Energy

Arrhenius equation is used to determine activation energy of adsorption (Arrhenius 1889). The Arrhenius equation is depicted by following equation (Chen *et al.* 2013):

$$\ln k_2 = \ln A - E_a / RT \quad (8.9)$$

Where k_2 (g mg $^{-1}$ min^{-1}) represents the rate constant obtained from the pseudo-second order kinetic model, E_a (J mol^{-1}) is the Arrhenius activation energy of adsorption and A is the Arrhenius factor. The slope of $-E_a/R$ is obtained by a plot between $\ln k_2$ against 1/T. The activation energy calculated is 32.32 kJ mol^{-1}.

8.8. Desorption experiments

Three desorbing agents namely HCl, HNO_3 and H_2SO_4 (0.1N for each solution) solutions were employed as desorbing agents for regeneration of adsorbent and reuse. The desorption efficiency was 54%, 48% and 52% for HCl, HNO_3, H_2SO_4 respectively. The HCl is used in regeneration studies. HCl (0.1N) solution can be used up to three cycles (Table 8.14).

Table 8.10 Cadmium removal after subsequent regeneration cycle (Initial concentration = 50 mg L^{-1}, pH = 7, Adsorbent dose = 4 g L^{-1}, Temperature = 303 K)

S.No.	Regeneration cycle	Cadmium removal (%) after regeneration cycle
1	1st	55.16
2	2nd	60.88
3	3rd	48.30

8.9. Conclusions

Cadmium was effectively removed from aqueous solutions using nanocrystalline iron oxide/hydroxide as an adsorbent. The adsorption equilibrium time was 20 min. The initial concentration of cadmium was most dominating factor for removal of cadmium using nano crystalline iron oxide/hydroxide. The most dominant factor initial concentration was followed by adsorbent dose and pH affecting adsorption of cadmium. Optimum parameters were initial concentration,

pH and adsorbent dose at 27 mg L^{-1}, 7 and 4 g L^{-1} respectively. The isotherm and kinetic models data fitted better with linear curve fitting analysis. The data for cadmium removal by nanocrystalline iron oxide/hydroxide follows Langmuir isotherm model and it followed a pseudo-second order kinetics. The change in Gibbs free energy was negative showing spontaneous nature of the adsorption process. The adsorption of cadmium using nanocrystalline iron oxide/hydroxide was endothermic in nature and occurred with increase of entropy. The regeneration of the adsorbent was done with hydrochloric acid (0.1 N) and showed steady results up to three regeneration cycles.